Cofilin and DNase I Affect the Conformation of the Small Domain of Actin

Irina V. Dedova,* Vadim N. Dedov,* Neil J. Nosworthy,* Brett D. Hambly,† and Cris G. dos Remedios*
*Muscle Research Unit, Institute for Biomedical Research, Department of Anatomy and Histology, and †Department of Pathology, The University of Sydney, NSW 2006, Australia

ABSTRACT Cofilin binding induces an allosteric conformational change in subdomain 2 of actin, reducing the distance between probes attached to Gln-41 (subdomain 2) and Cys-374 (subdomain 1) from 34.4 to 31.4 Å (pH 6.8) as demonstrated by fluorescence energy transfer spectroscopy. This effect was slightly less pronounced at pH 8.0. In contrast, binding of DNase I increased this distance (35.5 Å), a change that was not pH-sensitive. Although DNase I-induced changes in the distance along the small domain of actin were modest, a significantly larger change (38.2 Å) was observed when the ternary complex of cofilin-actin-DNase I was formed. Saturation binding of cofilin prevents pyrene fluorescence enhancement normally associated with actin polymerization. Changes in the emission and excitation spectra of pyrene-F actin in the presence of cofilin indicate that subdomain 1 (near Cys-374) assumes a G-like conformation. Thus, the enhancement of pyrene fluorescence does not correspond to the extent of actin polymerization in the presence of cofilin. The structural changes in G and F actin induced by these actin-binding proteins may be important for understanding the mechanism regulating the G-actin pool in cells.

INTRODUCTION

Changing dynamics of actin cytoskeleton assembly play an important role in a variety of eukaryotic cell functions such as division, differentiation, and particularly in cell motility driven by actin assembly. Populations of actin filaments in vivo turn over approximately two orders of magnitude more rapidly than is observed in vitro (Zigmond, 1993).

A number of small actin-binding proteins (ABPs) appear to control actin assembly and disassembly. They do this by altering the critical concentration of actin (the unpolymerized actin concentration present when F actin is formed) and/or by changing the kinetics of polymerization (Weber, 1999).

Monomeric or G actin has been the subject of intensive investigations and represents a substantial body of literature (Sheterline et al., 1999). It has a molecular mass of 43 kDa and dimensions of $67 \times 40 \times 37$ Å. The structure is divided into two major domains by a cleft containing a bound nucleotide and divalent cation (Fig. 1). Even though there is only a small difference in size in these domains, they are generally referred to as the large and small domains. This distinction is based on an early reconstruction of actin monomers (dos Remedios and Dickens, 1978). Several atomic structures (Kabsch et al., 1990; McLaughlin et al., 1993; Schutt et al., 1993) have revealed that the small and large domains each comprise two subdomains. Our interest is in subdomains 1 and 2 of the small domain.

Cofilin belongs to the actin depolymerizing factor (ADF)/cofilin family of ubiquitous, essential proteins that control actin assembly and the turnover rate of actin filaments (Lappalainen and Drubin, 1997; Rosenblatt et al., 1997; Bamburg, 1999; Carlier et al., 1999; McGough et al., 2001). Cofilin binds stoichiometrically to both monomeric and polymeric actin (Nishida et al., 1984). The interaction of cofilin with actin is pH dependent, suggesting that actin dynamics may be regulated by intracellular pH in vivo (Yonezawa et al., 1985; Hawkins et al., 1993; Hayden et al., 1993; Du and Frieden, 1998). The effects of cofilin in promoting actin assembly and disassembly can be explained by an acceleration of the turnover rate of actin (treadmilling

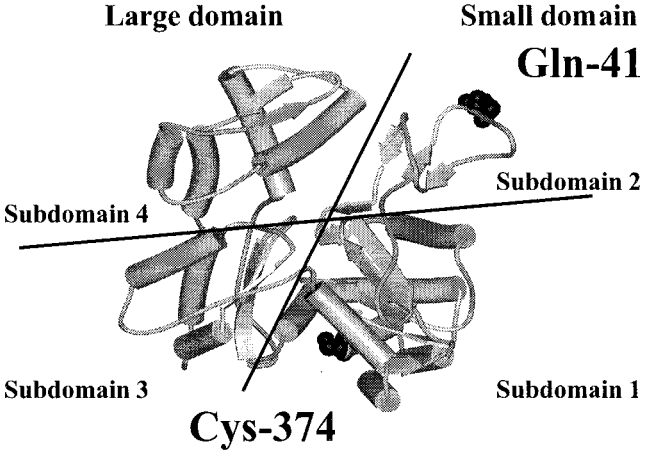

FIGURE 1 Ribbon representation of the actin monomer structure (Kabsch et al., 1990). The columns represent α-helices and arrows are β-sheets. Actin can be divided into the large and small domains, each of which is further divided into the subdomains 1 and 2 (within the small domain) and 3 and 4 (within the large domain). Black spheres indicate sites where fluorescent labels are attached to Gln-41 at the DNase I-binding loop in subdomain 2, and Cys-374 at the C-terminus in subdomain 1.

Submitted September 25, 2001, and accepted for publication February 22, 2002.

Address reprint requests to Cris G. dos Remedios, Institute for Biomedical Research, University of Sydney, Sydney, NSW 2006, Australia. Tel.: 61-2-93513209; Fax: 61-2-93152813; E-mail: crisdos@anatomy.usyd.edu.au.

0006-3495/02/06/3134/10 $2.00

or head-to-tail assembly) (Carlier et al., 1997; Didry et al., 1998; McGough et al., 2001). Others have suggested that cofilin depolymerizes by severing filaments and capping their barbed ends (Theriot, 1997; Bonet et al., 2000; Ichetovkin et al., 2000). Cofilin can also bind G actin at equimolar ratios, forming a nonpolymerizable complex (Du and Frieden, 1998). The G actin pool in embryonic skeletal muscle is controlled by ADF/cofilin as well as by profilin and thymosin (Nagaoka et al., 1996; Obinata et al., 1997).

The binding site for cofilin on F actin lies between two longitudinal actin subunits. It makes contact with subdomains 1 and 3 of the upper actin and subdomains 1 and 2 of the lower monomer. Cofilin changes the twist of F actin resulting in much shorter actin crossovers and loss of the phalloidin-binding site (McGough et al., 1997).

The precise binding location of cofilin on G actin is currently unknown because there is no crystal structure of an actin-cofilin complex. Cofilin competes with gelsolin segment-1 and profilin, both of which bind between actin subdomains 1 and 3 although to slightly different positions (McLaughlin et al., 1993; Schutt et al., 1993; McGough et al., 2001). Chemical cross-linking (Muneyuki et al., 1985), mutagenesis (Moriyama et al., 1992), and competitive binding by myosin and tropomyosin (Nishida et al., 1984) also suggest subdomain 1 as the most probable site for cofilin binding. Cofilin does not appear to undergo conformational changes when it binds to G or F actin (McGough et al., 2001). Nevertheless, the impact of cofilin on actin filament dynamics and structure suggests it induces a conformational change in actin.

Lazarides and Lindberg (1974) were the first to suggest that DNase I may be a cytoskeletal protein, whose primary function is related to the formation and function of actin filaments rather than to the degradation of DNA.

Stoichiometric interaction of DNase I with monomeric actin prevents actin polymerization and inhibits DNase I activity by binding to subdomains 2 and 4 (Mannherz et al., 1980; Kabsch et al., 1990). DNase I binds to residues 38 to 52 in subdomain 2 and may alter the structure of this region (Sheterline et al., 1999). Previous crystallographic, biochemical, and spectroscopic investigations suggest that G actin can alter its conformation due to interaction with actin-binding proteins (Page et al., 1998). Actin domains can still rotate relative to each other when certain ABPs bind (Schutt et al., 1993; Chik et al., 1996).

Intramolecular changes in the G actin structure induced by DNase I have been investigated previously by fluorescence resonance energy transfer spectroscopy (FRET). However, these data are controversial. The distance between the C-terminal Cys-374 (subdomain 1) and Gln-41 (subdomain 2) was reported to increase by 3 Å when DNase I binds (dos Remedios et al., 1994). However, Moraczewska et al. (1996) reported a smaller (1 Å) change in this distance when DNase I was bound. The probable explanation for this difference is in the high purity (protease-free) DNase I in the later report. Actin can form a ternary complex with DNase I and cofilin that is more stable than either binary complex (Kekic et al., 2001).

Here we use fluorescence spectroscopy to probe changes in the actin monomer when binary or ternary complexes are formed. Our results suggest that actin-binding proteins, such as cofilin and DNase I, induce dynamic and allosteric conformational changes in the small domain of actin.

MATERIALS AND METHODS

Reagents

Dansyl cadaverine (DC) and *N*-(1-pyrenyl)iodoacetamide (pyrene) were purchased from Molecular Probes Inc (Eugene, OR) *N*-{4-(dimethylamino)-3,5-dinitrophenyl}-maleimide (DDPM) was from Aldrich Chemical Co. (Milwaukee, WI). All other chemicals were purchased from Sigma (St. Louis, MO).

Proteins

Rabbit skeletal muscle actin was prepared according to the method described by Spudich and Watt (1971) with slight modification (Barden and dos Remedios, 1984) and used (unless otherwise stated) in G buffer (2 mM Tris-Cl, pH 8.0, 0.2 mM ATP, 0.2 mM dithiothreitol (DDT), 0.2 mM $CaCl_2$). Sephadex G-200 was used for the final step of purification. Before use, actin was clarified by centrifugation for 60 min at 100,000 $\times$ *g*. The concentration of actin was determined spectrophotometrically using an extinction coefficient of 0.63 cm^{-1} (0.1%, 290 nm). ATP-G-actin concentrations used for FRET experiments were 2 to 5 μM.

Cofilin was prepared as a recombinant protein using a cDNA sequence derived from chick embryo and kindly supplied by Dr. Takashi Obinata (Chiba, Japan). The protein was expressed in *Escherichia coli* using a *pGEX* plasmid and isolated by affinity chromatography. The resulting cofilin was obtained with a purity of >95% and its concentration was determined using an extinction coefficient of 0.98 cm^{-1} (0.1%, 280 nm). Bovine pancreatic DNase I (DPRF grade) was obtained from Worthington Biochemical Corporation (Lakewood, NJ). DNase I concentrations were determined using an extinction coefficient of 1.1 cm^{-1} (0.1%, 280 nm). All the actin, cofilin and DNase I samples were dialyzed against appropriate buffer overnight and centrifuged before the protein concentrations were obtained and fluorescence experiments were performed.

Gel electrophoresis

The native polyacrylamide gel electrophoresis (PAGE) gels comprised a 10% polyacrylamide running gel with a 4% stacking gel prepared according to (Laemmli, 1970) without addition of sodium dodecyl sulfate (SDS). The running buffer contained 0.2 mM ATP and 0.2 mM $CaCl_2$. Protein samples were mixed with an equal volume of loading buffer (62.5 mM Tris-Cl, pH 6.8, 10% glycerol, and 0.1% bromophenol blue) and run at low voltage packed on ice.

Labeling of actin with fluorescent probes

A donor probe, DC, was enzymatically bound to Gln-41 (Takashi, 1988; Moraczewska et al., 1996). G actin (2.5 mg/mL) was incubated with microbial transglutaminase at 1:50 molar ratio (actin:transglutaminase) and 10-fold molar excess of the DC probe over actin in a buffer containing 5 mM Tris-Cl, pH 7.7, 0.4 mM ATP, 0.5 mM $CaCl_2$, and 1 mM DDT. After overnight incubation on ice, the mixture was brought to room temperature,

and EGTA was added to a final concentration of 1 mM. Actin was polymerized by addition of 50 mM KCl and 2 mM $MgCl_2$ and collected by centrifugation at 100,000 × *g* for 90 min. F actin was exhaustively dialyzed against G buffer. Unbound label was removed by passing actin though Sephadex G-50 spin columns. The concentration of the covalently attached DC dye was calculated using an extinction coefficient of 4600 M^{-1} cm^{-1} at 330 nm (Molecular Probes). The labeling ratio of six different preparations was between 0.63 and 0.9.

DC-G-actin was further labeled at Cys-374 with a nonfluorescent acceptor, DDPM, according to (Miki, 1991). The labeling buffer contained 2 mM Tris-Cl, pH 8.0, 0.5 mM ATP, and 0.1 mM $CaCl_2$. After incubation with fivefold molar excess of the label overnight on ice, the reaction was terminated by addition of 1 mM β-mercaptoethanol. Actin was passed through a polymerization-depolymerization cycle with a final step of gel filtration though Sephadex G-50. The labeling ratio was calculated using an extinction coefficient of DDPM of 3050 M^{-1} cm^{-1} at 440 nm (Molecular Probes). The labeling ratio was 0.5 to 0.85 in six independent preparations.

Concentrations of labeled samples were determined by the Bradford assay. To determine the degree of DC labeling in the double-labeled actin, it was digested by trypsin. The procedures for tryptic digest and normalization of the spectra are described by Moraczewska et al. (1996). Actin was mixed with trypsin at 1:10 molar ratio and left overnight at 4°C. Digestion was stopped by 4 M excess of soybean trypsin inhibitor. As the result of fragmentation by trypsinolysis, donor and acceptor were separated, and fluorescence intensity was measured again in the presence of 1% sodium dodecyl sulfate.

Actin was labeled with *N*-(1-pyrenyl)iodoacetamide (pyrene) according to the method described by Kouyama and Mihashi (1981) with modifications. A 1.2-M excess of pyrene was added to G actin (3–4 mg/mL) in the presence of 0.5 mM ATP. It was immediately polymerized with 100 mM KCl and 2 mM $MgCl_2$ and incubated for 2 h at room temperature in the dark. Pellets were collected by centrifugation at 100,000 × g for 90 min. After depolymerizing against G buffer, actin was passed though Sephadex G-25 column. The extent of pyrene labeling was determined using the extinction coefficient of 26,000 M^{-1} cm^{-1} at 344 nm (Molecular Probes). The concentration of actin was determined by Bradford assay using bovine serum albumin as the standard. The labeling ratio was 0.6 to 0.9 for eight independent preparations.

Actin polymerization and pelleting assay

Actin was polymerized in the presence of various ratios of cofilin by the addition at time zero of 50 mM KCl and 2 mM $MgCl_2$. Binding of cofilin to F actin was examined by a pelleting assay. Samples were centrifuged at 100,000 × g for 90 min. 12% SDS PAGE gels were performed on pellets, supernatants, and samples before spinning. Gels were stained with Coomassie blue, and the intensities of the stained bands were determined by scanning gels with a densitometer. The absorption at 290 and 344 nm was also taken to compare the label content in the samples before and after the spin.

Fluorescence spectroscopy

Fluorescence measurements were carried out on an SLM 48000™S Multiple Frequency Lifetime Spectrofluorometer operating on xenon arc lamp at constant temperature (22°C). FRET experiments were carried out essentially as described previously by Moraczewska et al. (1996). Briefly, DC- and DC/DDPM-labeled G actin was excited at 332 nm in a temperature-controlled cuvette. Emission spectra, both in the presence and in the absence of the acceptor, were recorded over the range 440 to 750 nm. The efficiency of FRET (E) was determined by measuring the fluorescence intensity of the donor (DC) in both the presence (F_{DA}) and the absence (F_D) of the acceptor (DDPM), according to Eq. 1

$$E = 1 - (F_{DA}/F_D)/\alpha, \quad (1)$$

in which α is the degree of labeling with the acceptor in the double-labeled actin.

Energy transfer from donor to acceptor is reciprocally related to the sixth power of the distance separating the probes given by Eq. 2

$$E = R_o^6/(R_o^6 + R^6), \quad (2)$$

in which R_o is the Förster critical distance at which transfer efficiency is equal to 50%, and R is the distance between the donor and acceptor probes. The R_o distance for DC and DDPM as a donor-acceptor pair was calculated to be 29 Å for ATP-G actin. All experiments were at least performed in triplicate and presented as mean ± SD.

Actin polymerization was followed by an increase of pyrene-labeled actin fluorescence (excitation and emission wavelengths were 365 and 386 nm, respectively) at constant temperature as described elsewhere (Nishida et al., 1984; Du and Frieden, 1998). Additionally, polymerization was followed using a light scattering assay (Nishida et al., 1984). Both the excitation and emission wavelengths were set at 500 nm.

Fluorescence quenching measurements were carried out at 22°C by adding aliquots of a concentrated solution of acrylamide to DC-G actin. The excitation wavelength was 332 nm, and the emission intensity was measured at 512 nm. The data were analyzed using Stern-Volmer plots according to equation Eq. 3

$$F_0/F = (1 + K_{sv}[Q]e^{v[Q]} \quad (3)$$

in which F_0 and F are the fluorescence intensities in the absence and presence of quencher, respectively. K_{sv} is the quenching constant and is denoted by $k_q\tau_0$ in which k_q is the rate constant for quenching and τ_0 is the fluorescence lifetime of the fluorophore in the absence of quencher. In the limit of low quencher concentration, the data can be analyzed by Eq. 4

$$F_0/F = 1 + K_{sv}'[Q] \quad (4)$$

in which K_{sv}' is the apparent Stern-Volmer constant obtained experimentally from a plot of F_0/F versus $[Q]$.

RESULTS

Cofilin induces an allosteric conformational change in actin that is reversed by DNase I binding

Fig. 2 *A* shows the corrected and averaged ($n = 5$) fluorescence emission spectra for DC-G-actin alone (black), for the cofilin-actin complex (blue), and after binding of DNase I to form a ternary complex with cofilin-actin (red). When saturating cofilin binds to DC-G actin (2.5 cofilin:1 actin) at pH 6.8 we observe a large increase (46.7 ± 3.7%; $p = 0.004$; $n = 5$) in fluorescence intensity together with a substantial blue shift (5–7 nm) of the emission maximum (blue curve in Fig. 2 *A*). Binding of DNase I to cofilin actin (molar ratio of cofilin:actin:DNase I is 2.5:1:1.5) to form the ternary cofilin-actin-DNase I complex (red curve in Fig. 2 *A*) essentially reverses the effects of cofilin alone causing a significant decrease in enhanced fluorescence intensity (31.5 ± 5.0%; $p = 0.006$; $n = 5$). Addition of saturating levels of cofilin (2.5 M excess of cofilin over actin) at pH

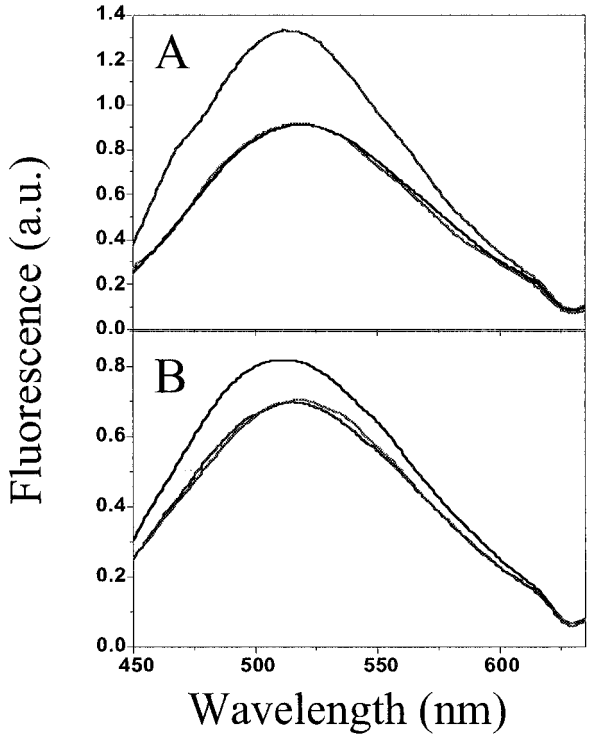

FIGURE 2 (*A*) Fluorescence emission spectra of DC-G-actin: in the absence of ABPs (*black curve*), in the binary cofilin-actin complex (*blue curve*), and in the ternary cofilin-actin-DNase I complex (*red curve*). Rabbit actin (2–5 μM) was dissolved in G buffer (2 mM Pipes, pH 6.8, 0.2 mM $CaCl_2$, 0.2 mM ATP, 0.2 mM DDT) in a temperature-controled cuvette at 22°C. The excitation wavelength was 332 nm. Cofilin and DNase I were added in 2.5 and 1.5 M excess over actin, respectively. Samples brought to the room temperature, mixed, and incubated for 10 min before spectra were taken and normalized (a.u., arbitrary units). (***B***) Fluorescence emission spectra of DC-G actin with the reverse sequence of ABPs addition: actin alone (*black curve*), DNase I-actin binary complex (*red curve*), and ternary DNase I-actin-cofilin complex (*blue curve*). Conditions were the same as described above.

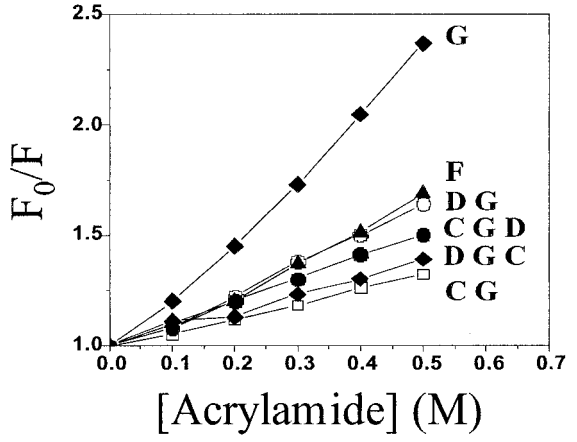

FIGURE 3 Stern-Volmer plots of acrylamide quenching data from: DC-G-actin (G curve, ■), F-actin (F curve, ▲), binary cofilin-actin complex (CG curve, □), binary DNase I-actin complex (DG curve, ○), ternary cofilin-actin-DNase I (CGD curve, ●), and ternary DNase I-actin-cofilin complex with the reverse order of ABPs addition (DGC curve, ◆). Actin, cofilin, and DNase I concentrations were 5, 12.5, and 7.5 μM, respectively.

8.0 induced changes in fluorescence intensity of DC actin that were less pronounced than at pH 6.8. The average increase in fluorescence intensity was 28.1 ± 4.8% (p = 0.01; n = 5) with a 4- to 7-nm blue shift of the emission maximum. DNase I binding to cofilin actin had essentially the same effect as observed at pH 6.8, largely reversing cofilin-induced changes of DC spectrum (data not shown).

Fig. 2 *B* illustrates the fluorescence emission spectra of DC-G actin at pH 6.8 with the order of ABPs addition reversed. DNase I causes a small decrease in fluorescence intensity (11 ± 1.9%; p = 0.008; n = 3) of the DC label (red curve in Fig. 2 *B*) and a slight red shift of the emission maximum. Binding of cofilin to the DNase I-actin-complex induces no further changes in this spectrum except for an insignificant blue shift (blue curve in Fig. 2 *B*). At pH 8.0, we observed the same changes (data not shown).

In the DNase I actin crystal complex Gln-41 makes intimate contact with DNase I (Kabsch et al., 1990). Cofilin is believed to bind subdomains 1 and 3 of G actin but does not bind subdomain 2 (Wriggers et al., 1998). Therefore, changes in fluorescent properties of the DC label attached to Gln-41 in subdomain 2 strongly suggest an allosteric modulation of actin structure. The augmentation of fluorescence intensity of the label suggests there is a cofilin-induced increase in hydrophobicity of the environment of Gln-41. However, if DNase I binds first, the spectral changes induced by cofilin are abolished, probably due to stabilizing effect of DNase I on the loop containing Gln-41.

Acrylamide quenching of DC-G actin in binary and ternary complexes with cofilin and DNase I

Quenching experiments were undertaken to confirm the relative inaccessibility of the DC probe in binary and ternary complexes. Acrylamide, an uncharged quencher, was incrementally (0–0.5 M) added to DC-G actin (Fig. 3) and Stern-Volmer plots generated (the ratio of initial and quenched fluorescence intensities, F_0/F versus quencher concentration). Quenching was linear, consistent with collisional quenching. The G-F transformation of actin is accompanied by a reduction (of ~50%) in quenching efficiency. This is consistent with Gln-41 residue being involved into actin-actin contacts in the filaments (Holmes et al., 1990). The DC probe was similarly inaccessible in all other binary and ternary complexes. The inaccessibility of Gln-41 in the DC-G-actin-cofilin complex is probably a consequence of an allosteric conformational change altering the Gln-41-containing loop, whereas the inaccessibility of the DC-G-actin-DNase I complex is probably due to the binding of DNase I directly to the loop containing Gln-41.

TABLE 1 Summary of changes in FRET between Gln-41 and Cys-374 of actin due to cofilin and/or DNase I binding

Sample	pH	Efficiency of FRET	R_o (Å)	R (Å)	ΔR (Å)
ATP-G actin	6.8 and 8.0	0.264 ± 0.04	29	34.4 ± 1.3	–
Cofilin actin	6.8	0.484 ± 0.038	31.03	31.4 ± 0.8	−3.0
	8.0	0.374 ± 0.05	30.3	33.0 ± 0.9	−1.4
DNase I actin	6.8	0.198 ± 0.021	28.13	35.5 ± 0.65	+1.1
	8.0	0.211 ± 0.028	28.4	35.4 ± 0.9	+1
Cofilin actin DNase I	6.8	0.161 ± 0.01	29	38.2 ± 0.5	+3.8
	8.0	0.193 ± 0.038	29.46	37.4 ± 1.3	+3.0
DNase I actin cofilin	6.8	0.137 ± 0.02	28.13	38.2 ± 1.1	+3.8
	8.0	0.158 ± 0.012	28.4	37.5 ± 0.7	+3.1

The procedures for FRET measurements and calculations are described in the Materials and Methods. Each type of the measurements has been performed at least five times using different preparations of proteins (see Results). The data are means ± SE (where appropriate). R_0 and R are the Föster critical distance and calculated interprobe distance, respectively; ΔR is the change in the distance due to ABPs binding at pH 6.8 and 8.0 compared with the distance in the actin alone.

Quantification of conformational changes using FRET

Using FRET spectroscopy we can determine both the direction and magnitude of a conformational change along the subdomain 1-subdomain 2 axis of the small domain (dos Remedios et al., 1994). We used the DC label on Gln-41 as a donor probe and placed a nonfluorescent acceptor (DDPM) at the single, highly reactive cysteine (Cys-374). The space-filled residues in Fig. 1 illustrate the locations of these sites. The R_0 (the Förster distance where transfer efficiency is 50%) for the donor (dansyl) and acceptor (DDPM) pair varies from 31.0 ± 0.3 Å (where the quantum yield of the donor is enhanced by cofilin binding) through to 28.1 ± 0.2 Å in the actin-DNase I complex (where the quantum yield is least). These data are summarized in the Table 1.

Fig. 4 demonstrates the emission spectra of the donor-labeled ATP-G actin in the presence of the acceptor (DC/DDPM actin) at pH 6.8. Fig. 4 *A* shows the spectrum when cofilin is added (cofilin:actin = 2.5:1) to form a binary complex (blue), and the spectrum when DNase I is subsequently added (red) to form the ternary complex (cofilin:actin:DNase I = 2.5:1:1.5). Fig. 4 *B* illustrates the formation of the ternary complex using the reverse order of ABPs addition (DNase I:actin:cofilin = 1.5:1:2.5). At first glance, these FRET spectra appear unremarkable in that none of the spectra are substantially different from each other. However, the blue and red spectral shifts reported for the donor only experiments are preserved. When measuring the fluorescence intensities to calculate the energy transfer efficiencies, a comparison was made between the donor intensity in the absence (Fig. 2) and in the presence of the acceptor (Fig. 4). For example, in the absence of acceptor, cofilin induces a large increase in fluorescence intensity and a blue shift (blue curve in Fig. 2 *A*), whereas in the presence of acceptor it causes no change in fluorescence intensity but a significant blue shift of emission spectrum (blue curve in Fig. 4 *A*). The differences in fluorescence intensities are due to changes in FRET efficiency between the donor and the acceptor.

At pH 6.8, the calculated FRET efficiency for the DC/DDPM probes pair for actin alone (black curves in Figs. 2 *A* and 4 *A*) is 0.264 ± 0.04, yielding a distance of 34.4 ± 1.3 Å between Gln-41 and Cys-374. This value is the same at

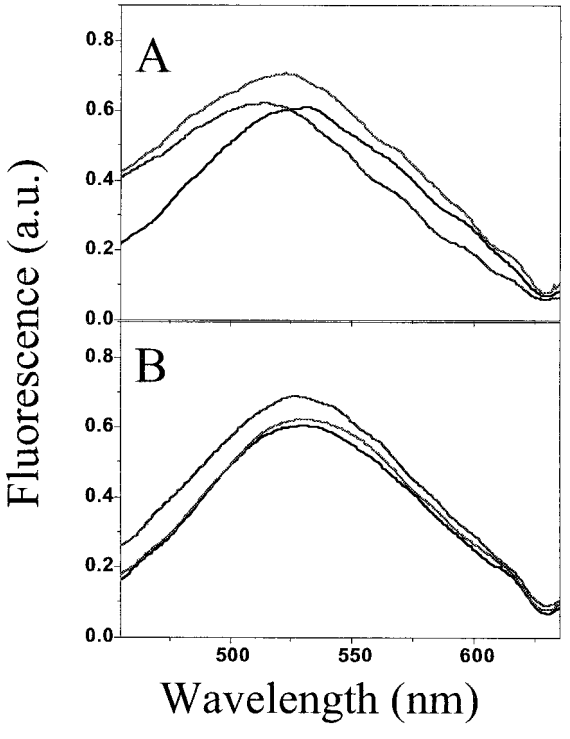

FIGURE 4 (***A***) Corrected fluorescence emission spectra of: DC-DDPM-G-actin (donor-acceptor labeled) in the absence of ABPs (*black curve*), the binary cofilin-actin (*blue curve*), and the ternary cofilin-actin-DNase I complexes (*red curve*). (***B***) Corrected fluorescence emission spectra of DC-DDPM-G actin when the order of ABPs addition is reversed: actin alone (*black curve*), DNase I-actin (*red curve*), and DNase I-actin-cofilin (*blue curve*). Protein concentrations and conditions are as described in Fig. 2. (a.u., arbitrary units).

pH 6.8 and 8.0 and is in good agreement with the recent distance reported for Ca-ATP-G actin (Moraczewska et al., 1996). Note that the fluorescence intensity of DC-DDPM-G actin (Fig. 4) is less than observed in Fig. 2 due to the transfer of energy between the donor and acceptor probes.

The difference in the fluorescence intensities in the presence and absence of acceptor when cofilin binds, corresponds to an increase in efficiency and a decrease of ~3 Å in the distance between the two probes (Table 1). Binding of DNase I to the cofilin-actin complex in the presence of acceptor results in a relatively large increase (8.8 ± 0.8%; $p = 0.001$; $n = 3$) in fluorescence intensity (red curve, Fig. 4 *A*). This is contrary to the significant 31.5% decrease seen in the absence of acceptor (red curve, Fig. 2 *A*). This decrease in FRET efficiency corresponds to a donor-acceptor distance of 38.2 ± 0.3 Å, corresponding to an increase of ~3.8 Å compared with the distance in actin alone (34.4 Å). Thus, cofilin decreases and DNase I increases the distance across the small domain of actin.

When the order of addition of cofilin and DNase I to G actin is reversed (Fig. 4 *B*), there are also corresponding changes in these donor-acceptor distances. In the presence of the acceptor, DNase I has almost no effect on the emission spectrum of DC-DDPM-actin (red curve, Fig. 4 *B*), but it causes a relatively large decrease in intensity in the absence of acceptor (red curve, Fig. 2 *B*). Thus, DNase I binding to G actin in the absence of cofilin results in a small increase in the distance between the probes (from 34.4–35.5 Å), consistent with our earlier observation using the same probe pair (Moraczewska et al., 1996). Cofilin binding (blue curve in Fig. 4 *B*) produces a further increase of 2.7 Å, yielding a final donor-acceptor distance for the ternary complex of ~38.2 Å. The final distance achieved in the ternary complex therefore remains unchanged (38.2 ± 0.6 Å) from the value obtained when cofilin was added first. We conclude that although the conformational changes in actin induced by DNase I alone are modest, they are significantly larger in the ternary complex. The order of ABPs addition does not affect the final distance.

Effects of pH on the magnitude of conformational change

The effects of cofilin on actin assembly are known to be pH dependent. The foregoing descriptions concern the effects of cofilin and DNase I on monomeric actin at pH 6.8. However, an equivalent set of experiments was also performed at pH 8.0 (Table 1). FRET data clearly indicate that the extent of the conformational changes in actin at basic pH is consistently smaller than observed at pH 6.8. The decrease in the distance induced by cofilin binding to actin is only ~1.4 Å compared with 3 Å at pH 6.8. In the presence of DNase I at pH 8.0 cofilin increases the distance by 2.1 Å, bringing the final value in the ternary complex to 37.5 Å. This distance is 0.7 to 0.8 Å ($p = 0.008$) shorter than at pH 6.8. Therefore, the effect of cofilin on actin structure is pH-sensitive with larger changes seen at lower pH. However, the effect of DNase I on the measured distance is modest (~1 Å) and does not depend on pH.

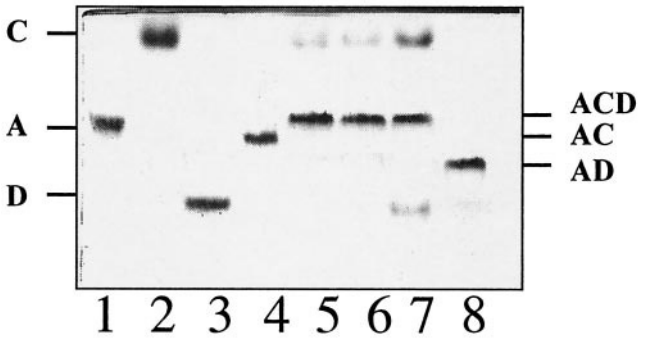

FIGURE 5 Native PAGE gel (10%) of DC-DDPM actin and its binary and ternary complexes with cofilin and DNase I. After performing FRET measurements experimental samples were mixed with the same volume of loading buffer containing no SDS. Mixtures were immediately electrophoresed on native gels as described in Materials and Methods. Contents of these gel lanes are: monomeric actin (lane 1), cofilin (lane 2), DNase I (lane 3), cofilin-actin (lane 4), ternary complex formed in order of addition cofilin, actin, then DNase I, where the ratio is 2.5:1:1.5 (lane 5); ternary complex formed in order of addition DNase I, actin, then cofilin, where the ratio is 1.5:1:2.5 (lane 6); ternary complex as described in lane 5 except molar ratio is now 10:1:5.5 (lane 7); and DNase I-actin (lane 8). The gel was stained with Coomassie blue.

Labeled actin forms a ternary complex with cofilin and DNase I

The ability of labeled actin to form binary and ternary complexes with ABPs can be demonstrated using native PAGE gels. The 10% native PAGE gel shown in Fig. 5 demonstrates that labeled actin alone forms a single band (lane 1), indicating an absence of oligomers. Cofilin and DNase I also form distinctive single bands seen in lanes 2 and 3, respectively. Binary complexes of cofilin-actin and DNase I actin are shown in lanes 4 and 8, respectively. Cofilin binds to monomeric actin without causing oligomerization (lane 4). Cofilin, DNase I, and actin are incorporated into the ternary complex with a 1:1:1 molar ratio in lanes 5, 6, and 7. In these lanes, we see no free actin monomer, indicating it has been entirely incorporated into the ternary complex regardless of the order of addition (compare lanes 5 and 6). The density of the band in the ternary complex is not altered by a large excess of cofilin and DNase I (lane 7). Therefore, the molar ratios of proteins used for FRET experiments are sufficient to achieve binary and ternary complexes in the absence of free actin. These data demonstrate that ternary complex formation reported elsewhere (Kekic et al., 2001) using unlabeled actin is unaffected by the presence of labels at Gln-41 and Cys-374.

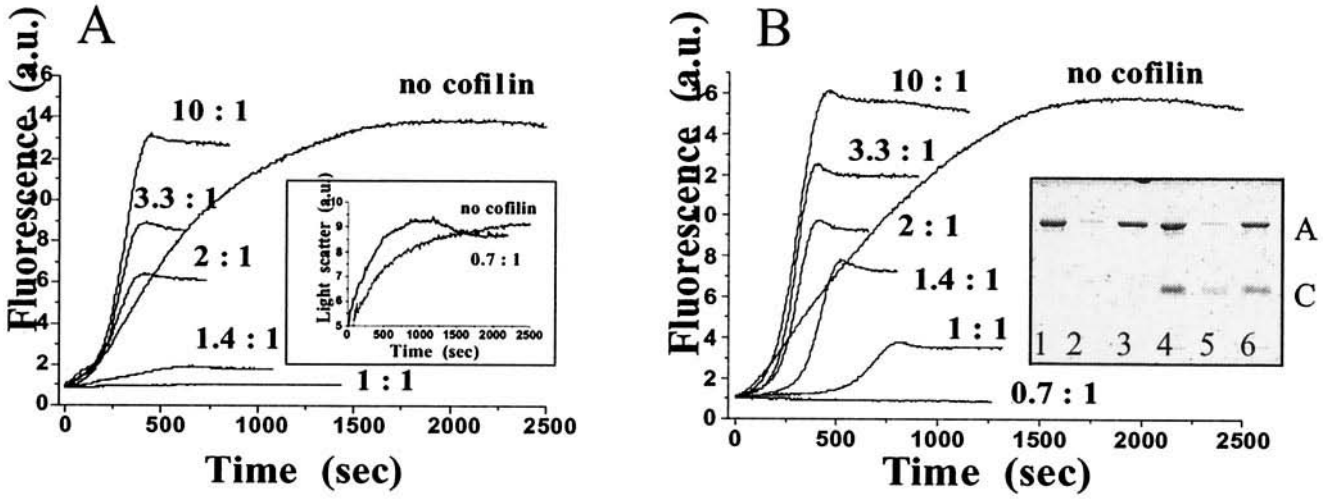

FIGURE 6 (***A***) Effect of cofilin on the time course of actin polymerization as measured by enhancement of pyrene fluorescence at pH 6.8. Actin was incubated with incremental molar ratios of cofilin prior to polymerization, which was initiated at zero time by addition of 50 mM KCl and 2 mM $MgCl_2$. The final actin concentrations remained constant (5 μM). The excitation and emission wavelengths were set at 365 and 386 nm, respectively. Temperature was kept constant (22°C). The molar ratios of actin to cofilin are shown next to the each curve. The inset figure shows effect of 1.5-fold excess of cofilin on actin polymerization measured by light-scattering. Unlabeled actin in G buffer (5 μM) was polymerized by addition of 50 mM KCl and 2 mM $MgCl_2$ in the absence ("no cofilin" curve) and presence of 7.5 μM cofilin (curve labeled 1.5:1). (***B***) Effect of cofilin on the time course of actin polymerization measured by pyrene fluorescence at pH 8.0. Molar ratios of actin to cofilin are shown next to the each curve. Experimental conditions are described in the legend of Fig. 6 *A*. F actin was centrifuged, and pellets and supernatants were analyzed by polyacrylamide gel electrophoresis (see Materials and Methods). The inset figure shows a 12% SDS PAGE gel of samples marked "no cofilin" and "0.7:1" after performing a pelleting assay: F actin in the absence of cofilin before the spin (lane 1), supernatant (lane 2) and pellet (lane 3) after the spin; F actin polymerized in the presence of 1.5 molar excess of cofilin before the spin (lane 4), and its supernatant (lane 5) and pellet (lane 6) after the spin.

Cofilin alters the conformation of the actin C terminus

We planned to monitor the assembly of labeled actin using fluorescence enhancement of the pyrene label bound to actin (Cys-374). However, at pH 6.8, stoichiometric cofilin binding abolished the fluorescence enhancement of pyrene actin monomers under conditions that induced actin polymerization. In the absence of cofilin, actin assembly follows the expected time course (see "no cofilin" curve, Fig. 6 *A*). Upon addition of cofilin, two effects were observed. First, at substoichiometric concentrations of cofilin, the rate of assembly is accelerated. Second, as the ratio of actin:cofilin is reduced from 10:1 to 1:1, the fluorescence enhancement declines until no change is observed at an equimolar ratio. A qualitatively similar effect is observed at pH 8.0 (Fig. 6 *B*) except there is an accentuated lag in the rise of fluorescence intensity.

Others have observed these effects (Du and Frieden, 1998) but have attributed the loss of pyrene fluorescence to the failure of actin to polymerize. However, we confirmed the polymerization of actin by monitoring light scattering (Fig. 6 *A*, inset), which compares the assembly of actin in the presence and absence of 1.5 M excess of cofilin over actin. The extent of polymerization is the same, but the rate is slightly faster. This result was also confirmed by sedimenting each sample in an Airfuge (100,000 × *g*, 15 min) and analyzing the pellets and supernatants by SDS PAGE (Fig. 6 *B*, inset).

The diminution in the pyrene fluorescence enhancement (Fig. 6, *A* and *B*) caused by cofilin binding may be due to a substantial shift in either the excitation or emission peaks as a consequence of that binding. Therefore, we examined the excitation and emission spectra for G and F actin and in binary and ternary complexes (Fig. 7, *A* and *B*, respectively). These spectra show two distinctive peaks using F actin, whereas the spectra of G actin are substantially reduced. In all cases, when cofilin is bound to actin, both spectra are essentially the same as observed for G actin and, particularly for G actin bound to DNase I. Thus, cofilin appears to lock the conformation of subdomain 1 surrounding Cys-374 into a G-like conformation.

DISCUSSION

In this paper we report distance measurements within the small domain of actin that alter substantially in response to the binding of ABPs. These conformational changes may be crucial in determining the role of the ABPs in regulating actin assembly. The ability of cofilin and DNase I to simultaneously attach to actin monomers is consistent with their binding to two separate parts of the molecule (Kekic et al., 2001). The cofilin-binding site includes a region near the N

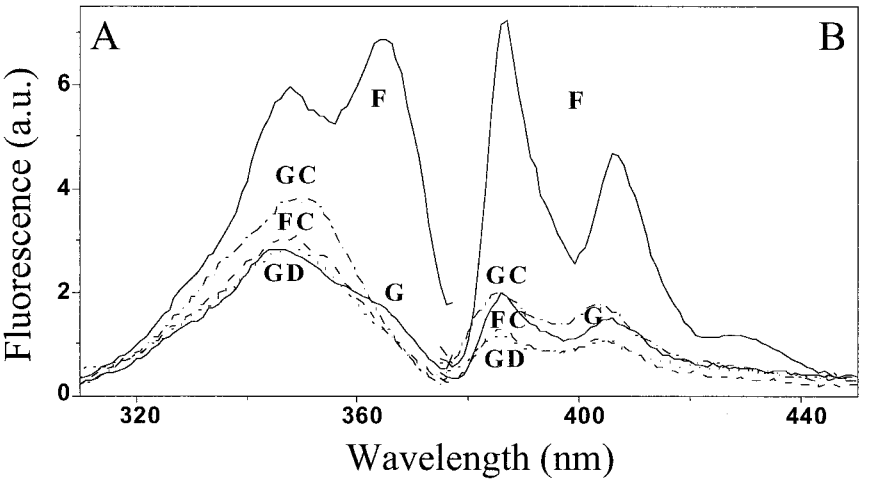

FIGURE 7 Effects of cofilin and DNase I on the excitation (*A*) and emission (*B*) spectra of pyrene-actin. Solid curves labeled "G" and "F" represent the excitation and emission spectra of controls, G, and F actin, respectively. Dash curves show the spectra of F actin in the presence of cofilin (FC); dash and dot, G actin in the presence of cofilin (GC); and dot curves, actin in the binary complex with DNase I (GD). The concentrations of actin, cofilin, and DNase I were 5, 12.5, and 7.5 μM, respectively.

and C termini of actin located in subdomain 1 (Muneyuki et al., 1985; Moriyama et al., 1992). This site is similar but not necessarily identical to the binding loci for depactin (Sutoh and Mabuchi, 1986), profilin (Schutt et al., 1993), and gelsolin segment 1 (Wriggers et al., 1998). DNase I binds to subdomains 2 and 4 (Kabsch et al., 1990).

Cofilin binding to subdomains 1 and 3 induces an allosteric conformational change that can be sensed at the distal end (Gln-41) of subdomain 2. The data supporting this conclusion are: 1) there is an allosteric change in subdomain 2 (Gln-41) when cofilin binds to subdomain 1; 2) cofilin binding to subdomain 1 is confirmed by a change in the local environment of a probe located at Cys-374 in the same subdomain; and 3) changes in FRET efficiency are consistent with changes in the distances between these two probes. Furthermore, the pH dependence of the FRET efficiencies is consistent with the pH-dependent effect of cofilin on actin assembly kinetics (for review, see Bamburg, 1999).

Previous observations have demonstrated that DNase I binding to subdomain 2 also induces an allosteric conformational change in subdomain 1 at the opposite end of the small domain. Crosbie et al. (1994) demonstrated the exposure of a new cleavage site for trypsin near the C terminus in the presence of DNase I. Also, binary complexes of actin with thymosin-β4, gelsolin segment 1, or profilin are dissociated when DNase I binds. This binding is negatively cooperative (Ballweber et al., 1997, 1998; Wriggers et al., 1998). On the other hand, we have reported that binding of cofilin to actin is enhanced in the presence of DNase I and vice versa (Kekic et al., 2001).

Kuznetsova et al. (1996) measured FRET efficiencies within subdomain 1 and observed a change when the DNase I-binding loop was cleaved. Truncation at the C terminus also reduces the rate of proteolytic cleavage of the DNase I-binding loop (Strzelecka-Golaszewska et al., 1995). The environmental sensitivity of the DC label has been used to detect allosteric structural changes before. Proteolytic removal of three amino acids from the C terminus of G actin resulted in a twofold decrease in the fluorescence intensity of the DC label (attached to Gln-41) (Moraczewska et al., 1996).

Allosteric conformational changes have also been detected in filamentous actin. Three-dimensional reconstructions of electron micrographs have visualized large allosteric effects involving the C terminus, the nucleotide-binding site, and the DNase I-binding loop (Egleman and Orlova, 1995). A similar finding was reported by Kim et al. (1996, 2000) who demonstrated that cleavage of the C-terminal two residues leads to a conformational change in the DNase I-binding loop. Intermolecular coupling between this loop (38–52) and subdomain 1 also play an important role in filament stability and sensitivity to gelsolin and myosin S1 binding (Khaitlina et al., 1993, 1997; Borovikov et al., 2000).

Simultaneous analysis of the four available crystal structures, combined with molecular simulations enabled Page et al. (1998) to conclude that subdomain 2 does not have a structural core and is intrinsically flexible. It can rotate independently of the other subdomains, all of which have rigid cores. Furthermore, the actin monomer structure may exist in two states, an "open" state where the nucleotide cleft opens by ~10° and a "closed" state where the cleft is more closed, similar to that defined for the actin-DNase I and F actin states. Contrary to its position in the open state, the DNase I-binding loop is folded "backwards" into subdomain 2 in the closed state (Page et al., 1998).

Our FRET data are also in a good agreement with the results of molecular dynamics simulation analysis by Wriggers et al. (1998), who modeled the structural changes in G actin when cofilin is docked onto the structure. Most of the changes were attributed either to a truncation of actin subdomains 2 and 4 or to cofilin-binding, which moves subdomain 1 towards cofilin by ~4 Å.

Otterbein et al. (2001) recently reported the structure of uncomplexed actin. They also emphasized that subdomain 2 undergoes an unexpected conformational change from an antiparallel β turn to an α-helix when ADP occupies the nucleotide cleft. The DNase I-binding loop undergoes a displacement of ~14 Å, but this is in a different plane to our FRET distance and consequently our FRET measurements would probably not sense the full magnitude of this change. We also showed that DNase I effectively reverses the cofilin-induced change in the environment of Gln-41. Thus, our observation of a 7-Å change between our FRET probes is consistent with this conformational mobility observed by x-ray diffraction.

The role of cofilin in inhibition or prevention of polymerization has been controversial. Many of these studies monitored polymerization using pyrene fluorescence. We show here that chicken embryonic cofilin accelerates polymerization of rabbit skeletal actin and does not significantly affect the extent of polymerization. However, cofilin binding to an actin monomer prevents pyrene fluorescence enhancement during polymerization, rendering pyrene ineffective for monitoring the extent of polymerization. The inhibition of pyrene fluorescence enhancement during polymerization seen upon cofilin binding is similar to the effect of myosin S1 on pyrene F actin, which quenches pyrene fluorescence by 70% (Kouyama and Mihashi, 1981).

In summary, our data point to the dynamic and flexible nature of subdomains 1 and 2 of actin. When ABPs form a complex they alter these subdomains, resulting in structures that either promote or inhibit polymerization. Interaction between these domains is allosteric. Such changes may be important in the regulation of actin assembly by these proteins.

We thank Dr. M. Miki and Dr. P. Moens for valuable comments. This research was supported by grants form the Australian Research Council and the National Health & Medical Research Council of Australia. I.D. received a scholarship from the National Health & Medical Research Council of Australia.

REFERENCES

Ballweber, E., K. Giehl, E. Hannappel, T. Huff, B. M. Jockusch, and H. G. Mannherz. 1998. Plant profilin induces actin polymerization from actin: β-thymosin complexes and competes directly with β-thymosins and with negative co-operativity with DNase I for binding to actin. *FEBS Lett.* 425:251–255.

Ballweber, E., E. Hannappel, T. Huff, and H. G. Mannherz. 1997. Mapping the binding site of thymosin beta4 on actin by competition with G-actin binding proteins indicates negative co-operativity between binding sites located on opposite subdomains of actin. *Biochem. J.* 327:787–793.

Bamburg, J. R. 1999. Proteins of the ADF/cofilin family: essential regulators of actin dynamics. *Annu. Rev. Cell Dev. Biol.* 15:185–230.

Barden, J. A., and C. G. dos Remedios. 1984. The environment of the high-affinity cation binding site on actin and the separation between cation and ATP sites as revealed by proton NMR and fluorescence spectroscopy. *J. Biochem.* 96:913–921.

Bonet, C., D. Ternent, S. K. Maciver, and A. Mozo-Villarias. 2000. Rapid formation and high diffusibility of actin-cofilin cofilaments at low pH. *Eur. J. Biochem.* 267:3378–3384.

Borovikov, Y. S., J. Moraczewska, M. I. Khoroshev, and H. Strzelecka-Golaszewska. 2000. Proteolytic cleavage of actin within the DNase-I-binding loop changes the conformation of F-actin and its sensitivity to myosin binding. *Biochim. Biophys. Acta.* 1478:138–151.

Carlier, M.-F., V. Laurent, J. Santolini, R. Melki, D. Didry, G X. Hong, N. H. Chua, and D. Pantanloni. 1997. Actin depolymerizing factor (ADF/cofilin) enhances the rate of filament turnover: implication in actin-based motility. *J. Cell Biol.* 136:1307–1322.

Carlier, M.-F., F. Ressad, and D. Pantaloni. 1999. Control of actin dynamics in cell motility: role of ADF/cofilin. *J. Biol. Chem.* 274: 33827–33830.

Chik, J. K., U. Lindberg, and C. E. Shutt. 1996. The structure of an open state of beta-actin at 2.65 Å resolution. *J. Mol. Biol.* 263:607–623.

Crosbie, R. H., C. Miller, P. Cheung, T. Goodnight, A. Muhlrad, and E. Reisler. 1994. Structural connectivity in actin: effect of C-terminal modifications on the properties of actin. *Biophys. J.* 67:1957–1964.

Didry, D., M.-F. Carlier, and D. Pantanloni. 1998. Synergy between actin depolymerizing factor/cofilin and profilin in increasing actin filament turnover. *J. Biol. Chem.* 273:25602–25611.

dos Remedios, C. G., and M. J. Dickens. 1978. Actin microcrystals and tubes formed in the presence of gadolinium ions. *Nature.* 276:731–733.

dos Remedios, C. G., P. C. Kiessling, and B. D. Hambly. 1994. DNase I binding induces a conformational change in the actin monomer. *In* Synchrotron Radiaton in the Bioscience. J. D. B. Chance, S. Ebashi, D. T. Goodhead, J. R. Helliwell, H. E. Huxley, T. Iizuka, J. Kirtz, T. Mitsui, E. Rubenshtein, N. Sakabe, T. Sasaki, G. Schmail, H. B. Stuhrmann, K. Wuthrich, and G. Zaccai, editors. Oxford University Press, New York. 418–425.

Du, J., and C. Frieden. 1998. Kinetic studies on the effect of yeast cofilin on yeast actin polymerization. *Biochemistry.* 37:13276–13284.

Egleman, E. H., and A. Orlova. 1995. Allostery, cooperativity, and different structural states in F-actin. *J. Struct. Biol.* 115:159–162.

Hawkins, M., B. Pope, S. K. Maciver, and A. G. Weeds. 1993. Human actin depolymerizing factor mediates a pH-sensitive destruction of actin filaments. *Biochemistry.* 32:9985–9993.

Hayden, S. M., P. S. Miller, A. Braunweiller, and J. R. Bamberg. 1993. Analysis of the interactions of actin depolymerizing factor with G- and F-actin. *Biochemistry.* 32:9994–10004.

Holmes, K. C., D. Popp, W. Gebhard, and W. Kabsch. 1990. Atomic model of the actin filament. *Nature.* 347:44–49.

Ichetovkin, I., J. Han, K. M. Pang, D. A. Knecht, and J. S. Condeelis. 2000. Actin filaments are severed by both native and recombinant dictyostelium cofilin but to different extents. *Cell Motil. Cytoskel.* 45:293–306.

Kabsch, W., H. G. Mannherz, D. Suck, E. F. Pai, and K. C. Holmes. 1990. Atomic structure of the actin: DNase I complex. *Nature.* 347:37–44.

Kekic, M., N. J. Nosworthy, I. Dedova, C. A. Collyer, and C. G. dos Remedios. 2001. Regulation of the cytoskeleton assembly: a role for a ternary complex of actin with two actin-binding proteins. *In* Molecular Interactions of Actin. Actin Structure and Actin-Binding Proteins. C. G. dos Remedios and D. D. Thomas, editors. Springer-Verlag, Heidelberg. 165–181.

Khaitlina, S., H. Hinssen, E. Kim E. Reisler, M. M. Tirion, D. ben-Avraham, M. Lorenz, and K. C. Holmes. 1997. Conformational changes in actin induced by its interaction with gelsolin: intermolecular coupling between loop 38-52 and the C-terminus in actin filaments: normal modes as refinement parameters for the F-actin model. *Biophys. J.* 73:929–937.

Khaitlina, S. Y., J. Moraczewska, and H. Strzelecka-Golaszewska. 1993. The actin/actin interactions involving the N-terminus of the DNase-I-binding loop are crucial for stabilization of the actin filament. *Eur. J. Biochem.* 218:911–920.

Kim, E., E. Reisler, M. M. Tirion, D. ben-Avraham, M. Lorenz, and K. C. Holmes 1996. Intermolecular coupling between loop 38–52 and the C-terminus in actin filaments: normal modes as refinement parameters for the F-actin model. *Biophys. J.* 71:1914–1919.

Kim, E., W. Wriggers, M. Phillips, K. Kokabi, P. A. Rubenstein, E. Reisler. 2000. Cross-linking constraints on F-actin structure. *J. Mol. Biol.* 299:421–429.

Kouyama, T., and K. Mihashi. 1981. Fluorimetry study of *N*-(1-pyrenyl)iodoacetamide-labelled F-actin. *Eur. J. Biochem.* 114:33–38.

Kuznetsova, I., O. Antropova, K. Turoverov, and S. Khaitlina. 1996. Conformational changes in subdomain I of actin induced by proteolytic cleavage within the DNase I-binding loop: energy transfer from tryptophan to AEDANS. *FEBS Lett.* 383:105–108.

Laemmli, U. K. 1970. Cleavage of structural proteins during the assembly of the head of bacteriophage T4. *Nature.* 227:680–685.

Lazarides, E., and U. Lindberg. 1974. Actin is the naturally occurring inhibitor of deoxyribonuclease I. *Proc. Natl. Acad. Sci. U.S.A.* 71: 4742–4746.

Lappalainen, P., and D. G. Drubin. 1997. Cofilin promotes rapid actin filament turnover in vivo. *Nature.* 388:78–82.

Mannherz, H. G., R. S. Goody, M. Konrad, and E. Nowak. 1980. The interaction of bovine pancreatic deoxyribonuclease 1 and skeletal muscle actin. *Eur. J. Biochem.* 104:367–379.

McGough, A., B. Pope, W. Chiu, and A. Weeds. 1997. Cofilin changes the twist of F-actin: implications for actin filament dynamics and cellular function. *J. Cell Biol.* 138:771–781.

McGough, A., B. Pope, and A. Weeds. 2001. The ADF/cofilin family: acceleration of actin reorganization in molecular interactions of actin. *In* Actin Structure and Actin-Binding Proteins. C.G. dos Remedios and D.D. Thomas, editors. Springer-Verlag, Heidelberg. 135–154.

McLaughlin, P. J., J. T. Gooch, H. G. Mannherz, and A. G. Weeds. 1993. Structure of gelsolin segment 1-actin complex and the mechanism of filament severing. *Nature.* 364:685–692.

Miki, M. 1991. Detection of conformational changes in actin by fluorescence resonance energy transfer between tyrosine-69 and cysteine-374. *Biochemistry.* 30:10878–10884.

Moraczewska, J., H. Strzelecka-Golaszewska, P. D. Moens, and C. G. dos Remedios. 1996. Structural changes in subdomain 2 of G-actin observed by fluorescence spectroscopy. *Biochem. J.* 317:605–611.

Moriyama, K., N. Yonezawa, H. Sakai, I., Yahara, and E. Nishida. 1992. Mutational analysis of an actin-binding site of cofilin and characterization of chimeric proteins between cofilin and destrin. *J. Biol. Chem.* 267:7240–7244.

Muneyuki, E., E. Nishida, K. Sutoh, and H. Sakai. 1985. Purification of cofilin, a 21,000 molecular weight actin-binding protein, from porcine kidney and identification of the cofilin-binding site in the actin sequence. *J. Biochem.* 97:563–568.

Nagaoka, R., N. Minami, K. Hayakawa, H. Abe, and T. Obinata. 1996. Quantitative analysis of low molecular weight G-actin-binding proteins, cofilin, ADF and profilin, expressed in developing and degenerating chicken skeletal muscles. *J. Muscle Res. Cell Motil.* 17:463–473.

Nishida, E., S. Maekawa, and H. Sakai. 1984. Cofilin, a protein in porcine brain that binds to actin filaments and inhibits their interactions with myosin and tropomyosin. *Biochemistry.* 23:5307–5313.

Obinata, T., R. Nagaoka-Yasuda, S. Ono, K. Kusano, K. Mohri, Y. Ohtaka, S. Yamashiro, K. Okada, and H. Abe. 1997. Low molecular-weight G-actin binding proteins involved in the regulation of actin assembly during myofibrillogenesis. *Cell Struct. Funct.* 22:181–189.

Otterbein, L., P. Graceffa, and R. Dominguez. 2001. The crystal structure of uncomplexed actin in the ADP state. *Science.* 80:705–708.

Page, R., U. Lindberg, and C. E. Schutt. 1998. Domain motions in actin. *J. Mol. Biol.* 280:463–474.

Rosenblatt, J., B. J. Agnew, H. Abe, J. R. Bamberg, and T. J. Mitchison. 1997. Xenopus actin depolymerizing factor/cofilin (XAC) is responsible for the turnover of actin filaments in Listeria monocytogenes tails. *J. Cell Biol.* 136:1323–1332.

Schutt, C. E., J. C. Myslik, M. D. Rozycki, N. C. Gooneskere, and U. Lindberg. 1993. The structure of crystalline profilin-beta-actin. *Nature.* 365:810–816.

Sheterline, P., J. Clayton, and J. Sparrow. 1999. Actin. *In Protein Profile*, 4th ed. P. Sheterline, editor. Oxford University Press, New York. 1–103.

Spudich, J. A., and S. Watt. 1971. The regulation of rabbit skeletal muscle contraction: I. Biochemical studies of the interaction of the tropomyosin-troponin complex with actin and the proteolytic fragments of myosin. *J. Biol. Chem.* 246:4866–4871.

Strzelecka-Golaszewska, H., M. Mossakowska, A. Wozniak, J. Moraczewska, and H. Nakayama. 1995. Long-range conformational effects of proteolytic removal of the last three residues of actin. *Biochem. J.* 307:527–534.

Sutoh, K., and I. Mabuchi. 1986. Improved method for mapping the binding site of an actin-binding protein in the actin sequence: use of a site-directed antibody against the N-terminal region of actin as a probe of its N-terminus. *Biochemistry.* 25:6186–6192.

Takashi, R. 1988. A novel actin label: a fluorescent probe at glutamine-41 and its consequences. *Biochemistry.* 2:938–943.

Theriot, J. A. 1997. Accelerating on a treadmill: ADF/cofilin promotes rapid actin filament turnover in the dynamic cytoskeleton. *J. Cell Biol.* 136:1165–1168.

Weber, A. 1999. Actin binding proteins that change extent and rate of actin monomer-polymer distribution by different mechanisms. *Mol. Cell. Biochem.* 190:67–74.

Wriggers, W., J. X. Tang, T. Azuma, P. W. Marks, and P. A. Janmey. 1998. Cofilin and gelsolin segment-1: molecular dynamics simulation and biochemical analysis predict a similar actin binding mode. *J. Mol. Biol.* 282:921–932.

Yonezawa, N., E. Nishida, and H. Sakai. 1985. pH control of actin polymerization by cofilin. *J. Biol. Chem.* 260:14410–14412.

Zigmond, S. H. 1993. Recent quantitative studies of actin filament turnover during cell locomotion. *Cell Motil. Cytoskel.* 25:309–316.